Ocular biometry in rabbits using computed tomography

Received: 10 August 2023 | Revised: 11 February 2024 | Accepted: 28 February 2024

DOI: 10.1111/vop.13209

ORIGINAL REPORT

WILEY

Ocular biometry in rabbits using computed tomography

Nicholas Goody[1] | **Nicolas Israeliantz**[1] | **Azzurra Massidda**[2] | **Jenna Richardson**[1] | **Benjamin Blacklock**[1] | **Jordan Mitchell**[3,4] | **Tiziana Liuti**[1]

[1]Royal (Dick) School of Veterinary Studies, Hospital for Small Animals, The University of Edinburgh, Midlothian, UK

[2]The Ralph Veterinary Referral Centre, Marlow, UK

[3]The Roslin Institute, The University of Edinburgh, Midlothian, UK

[4]Department of Pathobiology and Population Sciences, Royal Veterinary College, Hertfordshire, UK

Correspondence
Nicholas Goody, Royal (Dick) School of Veterinary Studies, Hospital for Small Animals, The University of Edinburgh, Easter Bush Campus, Midlothian, EH25 9RG, UK.
Email: s0811094@ed.ac.uk

Abstract

Objective: To describe a repeatable method of measuring ocular structures and to establish ocular biometry reference ranges in adult domestic rabbits (*Oryctolagus cuniculus*) without medical history or imaging findings consistent with ophthalmic disease using a 64-slice multidetector computed tomography scanner.

Procedure: In this retrospective and observational anatomic study, 100 eyes from 50 rabbits without medical history or imaging findings consistent with ophthalmic disease who received a head computed tomography scan were selected for measurement of globe length, width, and height using 3D multiplanar reconstruction. Lens width and length, the anteroposterior length of the anterior and vitreous chambers, and attenuation of the lens and vitreous chamber were collected. These parameters were compared against age, sex, weight, body condition, and ear conformation.

Results: A reference guide was established, with globe width being the largest dimension (18.03 ± 0.81 mm), followed by height (17.18 ± 0.69 mm) and then length (16.64 ± 0.66 mm). Increased weight was associated with an increase in globe height ($p = 2.43 \times 10^{-5}$), length ($p = 1.63 \times 10^{-4}$), and width ($p = 7.0 \times 10^{-3}$). Increased age was associated with increased lens attenuation ($p = 1.28 \times 10^{-7}$) and increased transverse lens width ($p = 1.64 \times 10^{-3}$). Inter- and intra-observer agreement was excellent.

Conclusions: CT is a reliable modality for measurement of ocular biometry dimensions in rabbits. These reference values can be applied to aid in identifying diseases that affect the dimensions of the ocular structures in rabbits over 18 months of age.

KEYWORDS

attenuation, dimensions, exotic, lens, reference range, vitreous chamber

1 | INTRODUCTION

The rabbit is the third most encountered pet in small animal veterinary practice in the United Kingdom.[1] The rabbit eye has historically been used as a model for human ophthalmologic research, due to comparative similarities to human eyes in corneal thickness, aqueous humor volume, aqueous production rate, tear volume,

and tear production rate.[2] Ocular biometry is the measurement of the dimensions of the ocular structures, and was previously determined in rabbits using cadavers.[3] The rabbit globe is described as a prolate spheroid in shape.[4]

As computed tomography (CT) scanners become more available in animal hospitals,[5] its use in rabbits is becoming more accessible, with several recent publications on normal anatomical structures and classification of cranial disease processes.[5–10] Rabbits frequently present for clinical problems related to dental and auricular disease.[6–11] The complex interdigitating structures of the head are well assessed using CT[12] and with the eyes included in those CT studies, there is a need for a standardized method of measurement, and reference ranges to assess ocular structures.

In other veterinary species, CT has been demonstrated to be a suitable modality for assessing ocular dimensions,[13–17] and has been demonstrated to aid in diagnosis of ophthalmologic disease, for example those involving anterior and posterior lens luxation, and changes in lens shape.[17] A reference range for normal CT ocular measurements in rabbits has not been established in literature. A reference range may be used to aid in diagnosis of conditions that affect ocular dimensions. The effect of ear conformation, body condition, age, and weight on ocular dimensions has not been investigated in rabbits.

The aims of this study were (i) to establish a reliable and repeatable method to measure ocular structures in a rabbit using CT, with high intra- and interobserver agreement; (ii) to establish a reference guide for globe length, height, and width, anteroposterior distance of the anterior chamber, anteroposterior distance of the vitreous chamber, lens size, and attenuation in Hounsfield Units (H.U.) of the vitreous humor and lens; (iii) to investigate the correlation between left and right ocular biometric measurements; (iv) to identify whether signalment features including age, ear conformation, body condition, weight and sex are associated with statistically significant variation in ocular biometric measurements; (v) to determine if intravenous contrast administration significantly affects measured dimensions or attenuation of ocular structures.

It was hypothesized that (i) there would be no statistically significant difference between the left and right ocular measurements, so that left and right eyes could be included together for analysis of a larger sample; (ii) among different sexes and ear conformations there would be no significant difference in measurements; (iii) as weight increases, so too would dimensions of the ocular structures similar to what was found in dogs[13]; (iv) body condition would not affect ocular dimensions, demonstrating that lean weight affects ocular dimensions rather than body condition[13]; (v) lens attenuation will increase with age secondary to increased likelihood of nuclear sclerosis.

2 | MATERIALS AND METHODS

2.1 | Sample

For this retrospective original mixed-methods (anatomic and observational) study, the electronic medical records of the Hospital for Small Animals of the Royal (Dick) School of Veterinary Studies were reviewed, and rabbits between 18 and 78 months of age that had a CT of the head between July 2017 and September 2020 for non-ophthalmologic reasons were selected based on convenience sampling. The study was approved by the Veterinary Ethical Review Committee of the Royal (Dick) School of Veterinary Studies (Veterinary Ethical Review Committee reference 145.20). Client consent for use of images and clinical data in research was granted for each case at admission to the university hospital.

Rabbits were only included if the review of their medical and imaging records did not reveal the presence of ocular or orbital pathology, any pathology causing mass effect over the maxillary or orbital region, mediastinal masses as a cause of exophthalmos,[18] and if the CT studies were of diagnostic quality. Medical data and signalment characteristics were recorded by a European board-certified exotics clinician (J.R.), who was blinded to the CT measurements. Data collected for each patient included ear conformation, age, sex, neuter status, weight, and body condition. Body condition was categorized as poor, average, or obese based on recorded body condition scores (scored out of five, with 1–2 being poor, 3 being average, and 4–5 being obese) and descriptions within medical records (scored as poor if prominent pelvic and vertebral bones were described on imaging reports or clinical examination, scored as obese if large amount of fat over the pelvic and vertebral bones were noted on imaging report or clinical examination). Ear conformation was recorded as upright or lop.

2.2 | CT measurements

Images were acquired using a 64-row multidetector computed tomography scanner (Somatom® Definition AS Siemens, Erlangen, Germany). CT Calibration using a phantom (Siemens CT Water Phantom, Erlangen, Germany) is performed once weekly. CT studies were performed in conscious animals, placed inside a VetCat Trap (Universal Medical Systems Inc., Solon, USA) plexiglass

tube in sternal recumbency (Figure 1). Scan settings included a pitch of 1.5, tube potential of 120 kVp, reference tube current of 160 mA, slice thickness of 1.0 mm and matrix 512 × 512. Only soft tissue algorithm reconstructions were assessed for the purposes of this study (Siemens proprietary kernel H40), and window width and window level were individually adjusted by the observers to optimize identification of structures (with a default soft tissue window width 350 HU, window level 40 HU). The images were uploaded to a central picture archiving and communication system (PACS).

To perform the measurements, images were reviewed on a computer workstation (Apple Mac Pro, Apple, USA) with a calibrated LCD flat screen monitor using dedicated DICOM viewer software (Horos, Purview, Annapolis MD, USA, version 3.3.6). Images were assessed using multiplanar reconstructions (MPRs) to maximize ocular dimensions. Firstly, transverse, sagittal, and dorsal planes of the head were obtained by adjusting the centers of rotation on the MPR, aligning them to the nasal septum (on the transverse and dorsal planes) and hard palate (on the sagittal plane). Then, first in the transverse and then in the dorsal planes of the head, the center of rotation was positioned immediately posterior to the lens at the slice of its maximal dimension (based on visual inspection), and subsequently rotated to align it with its axial length and transverse width. This resulted in images of the transverse, parasagittal, and dorsal planes of the globe.

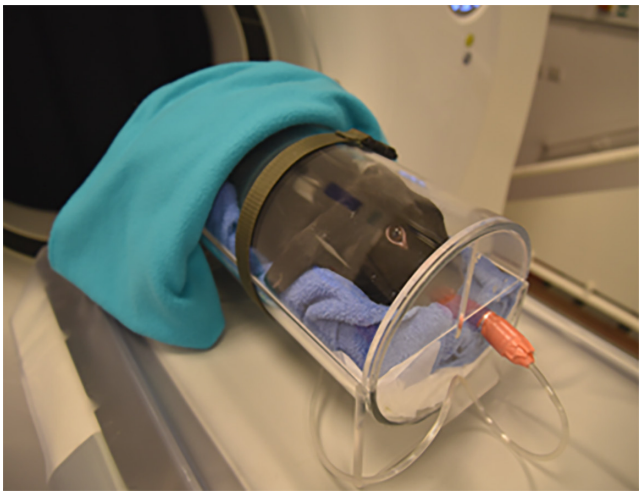

FIGURE 1 A conscious rabbit placed in sternal recumbency within the VetCat Trap plexiglass tube.

Multiple dimensions of both eyes ($n = 100$) were assessed on the pre-contrast CT images. All measurements were performed by a third-year diagnostic imaging resident (N.I.), who was blinded to signalment data, and the right eye was always measured first to maintain consistency. For each dimension, the maximal distance was determined by visual judgment:

1. Globe length from the external margin of the cornea to the internal margin of the retina–choroid–sclera complex at the maximum antero-posterior dimension along a line perpendicular to and bisecting the lens measured in a parasagittal plane (Figure 2A).
2. Globe height from the internal margin of the retina–choroid–sclera complex to the internal margin of the retina–choroid–sclera complex of the opposite side, at the maximal distance posterior and parallel to the lens measured in a parasagittal plane (Figure 2A).
3. Globe width from the internal margin of the retina–choroid–sclera complex to the internal margin of the retina–choroid–sclera complex of the opposite side, at the maximal distance posterior and parallel to the lens measured in adorsal plane (Figure 2B).
4. Anteroposterior distance of the lens (axial length) from the anterior surface to the posterior surface of the lens measured in aparasagittal plane (Figure 3A).
5. Lateromedial distance of the lens (transverse width) taken at its widest dimension measured in adorsal plane (Figure 3B).

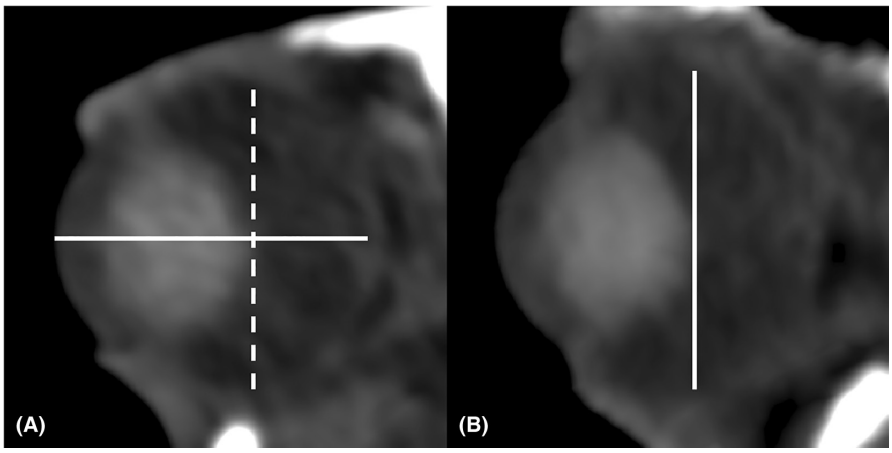

FIGURE 2 Pre-contrast computed tomographic multiplanar reconstructions in soft tissue algorithm of the head of a rabbit aligned to assess the ocular structures, showing globe measurements of length (solid line) and height (dotted line) on parasagittal (A), and width (solid line) on dorsal (B) planes of the globe.

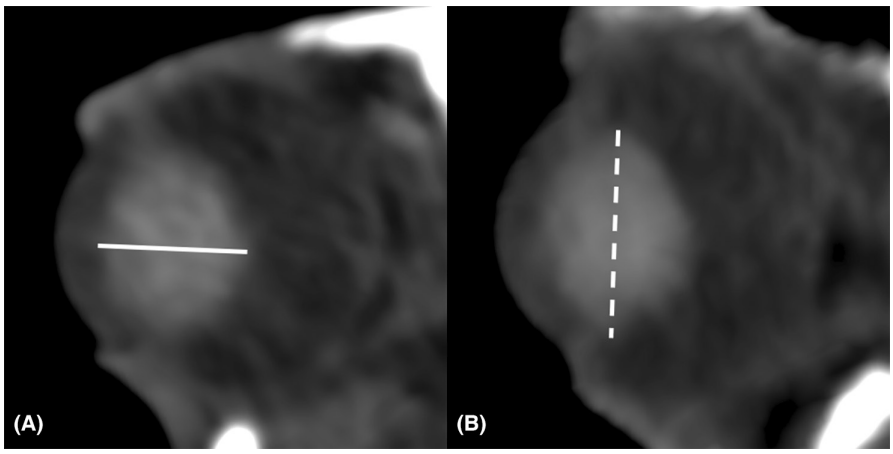

FIGURE 3 Pre-contrast computed tomographic multiplanar reconstructions in soft tissue algorithm of the head of a rabbit aligned to assess the ocular structures, showing lens measurements of axial length (solid line) on parasagittal (A), and transverse width (dotted line) on dorsal (B) planes of the globe.

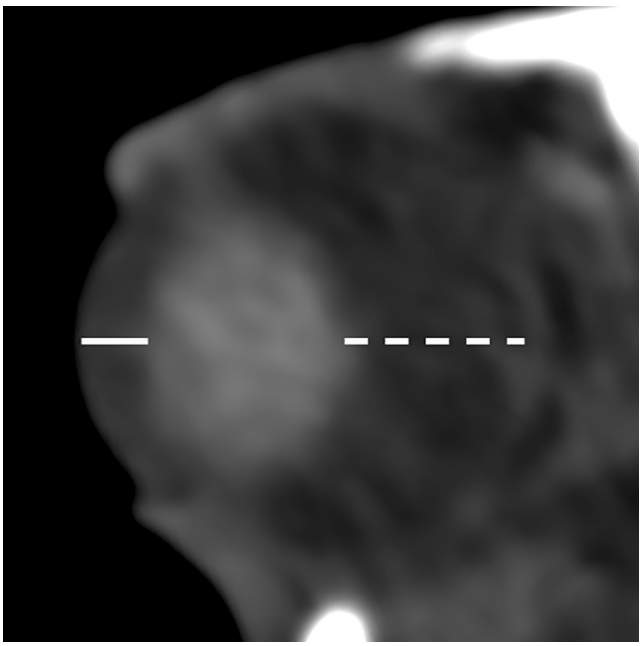

FIGURE 4 Pre-contrast computed tomographic multiplanar reconstructions in soft tissue algorithm of the head of a rabbit aligned to assess the ocular structures, showing the measurements of anterior chamber length (solid line) and vitreous chamber length (dotted line) in aparasagittal plane.

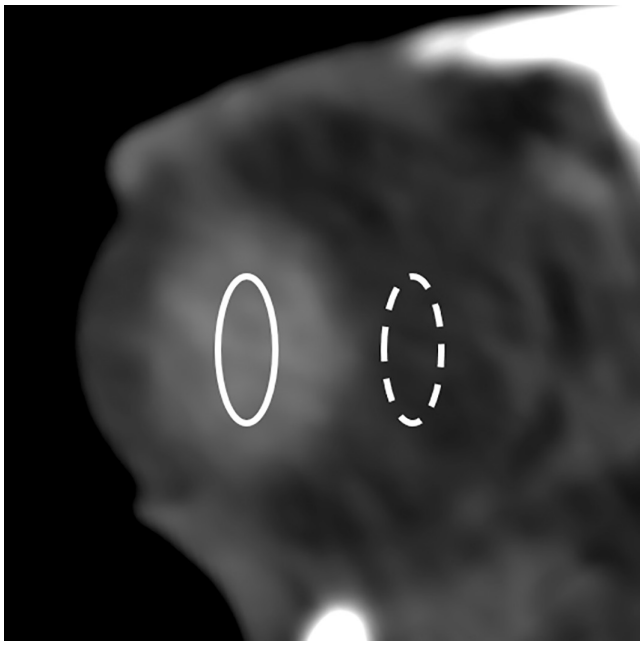

FIGURE 5 Pre-contrast computed tomographic images of the rabbit eye in which measurement of attenuation (Hounsfield units) of the lens (solid line) and vitreous chamber (dotted line) are performed by drawing a region of interest in the center of these structures in aparasagittal plane.

6. Anteroposterior distance of the anterior chamber, from the external margin of the cornea to the anterior surface of the lens measured in a parasagittal plane (Figure 4).
7. Anteroposterior distance of the vitreous chamber, from the posterior surface of the lens to the internal surface of the retina–choroid–sclera complex measured in a parasagittal plane (Figure 4).
8. Mean attenuation in H.U. of the vitreous and lens by drawing a region of interest in the center of these structures in a parasagittal plane, while taking care to avoid the edges (to avoid averaging artifact), and areas of beam hardening artifact when present (Figure 5).

2.3 | Comparison of CT measurements before and after contrast administration

A subset of 10 rabbits (20 eyes) was selected randomly from the group of 50, and was used to determine the influence of intravenous contrast medium administration on ocular measurements. The same measurements were performed by the same observer on images acquired 18 s after intravenous contrast medium administration (2 mL/kg of Iopamidol, Niopam 350, Bracco UK Ltd at a 0.8 mL/min rate) through an intravenous cannula placed in the lateral marginal auricular vein by a power injector pump

(CT Exprès™ Injector Unit, Bracco Ingineering S.A., Lausanne, Switzerland).

2.4 | Intra- and interobserver repeatability

The same subset of 10 rabbits (20 eyes) was utilized to assess intra- and interobserver agreement. The ocular structures of these rabbits were measured three times by the first observer, a diagnostic imaging resident in their third year of training (N.I.), at intervals of at least 2 weeks between measurements. A second observer, a European College of Veterinary Diagnostic Imaging board-certified radiologist (T.L.), performed all measurements once, unaware of the results of the first observer and blinded to the signalment data. MPR from the original transverse images was performed by each observer each time the structures were measured.

2.5 | Statistical analysis

Summary statistics (mean, standard deviation, median, and range) for ocular biometric data were calculated for left and right eyes individually, as well as for both eyes combined. Data were plotted to evaluate the distribution and to inform the selection of parametric or non-parametric statistical tests as appropriate. To determine the correlation between right and left ocular biometrics, Pearson's correlation coefficient was calculated for all nine parameters.[19] For each ocular biometric, multivariate linear mixed-effect models were run to identify whether age, ear conformation, sex, body condition or weight were associated with differences in measurements, with left and right ocular data combined. Pre- and post-contrast measurements were compared by Wilcoxon signed-rank test. Intra- and interobserver repeatability were calculated as a single fixed rater intraclass correlation coefficient (ICC), directly comparing each data point of all measurements made by each observer. All statistical analyses were performed using RStudio (R Core Team 2019), and statistical significance was set to $p < .05$.

3 | RESULTS

Fifty rabbits (100 eyes) were retrospectively assessed. Twenty-one were female (six entire, 15 neutered) and 29 were male (five entire, 24 neutered). Twenty-two were upright-eared, 28 were lop-eared. Mean age was 41 months (SD 15.05), and mean weight was 2.4 kg (SD 0.65). Twenty-six rabbits had average body condition, 10 were obese, and 13 had poor body condition. The body condition for one rabbit was not available in the medical records.

3.1 | Summary measurements for biometric data

Summary of ocular structure measurements from all 50 rabbits are presented in Table 1. The width was the largest dimension (18.03 ± 0.81 mm), followed by the height (17.18 ± 0.69 mm) and then the length (16.64 ± 0.66 mm). The length of the vitreous chamber was on average almost three times larger than that of the anterior chamber.

3.2 | Correlation between left and right ocular measurements

For parameters pertaining to measured distances (globe length, width, and height, anterior chamber and vitreous chamber lengths, and lens length and width) there was statistically significant moderate to strong linear positive correlation between the right and left ocular measurements (Pearson's $r = .45–.71$, $p \leq .001$), demonstrating that as ocular structures in one eye increased, there was a proportional increase in structures in the other eye. Both right and left eyes were included in the sample. For measurement of mean lens attenuation there was a positive correlation ($r = .37$, $p = .008$). There was no statistical correlation between the left and right eye mean vitreous attenuation ($r = .07$, $p = .64$).

3.3 | Association between ocular biometrics and sex, ear conformation, body condition, weight, and age

Summary statistics for the 49 rabbits with all variables recorded and compared against nine biometric parameters are presented in Table 2. One rabbit was excluded, because it did not have available body condition data. No correlation was observed between biometric measurements and body condition score.

Increased weight was statistically associated with an increase in the globe height ($p = 2.43 \times 10^{-5}$), anteroposterior globe length ($p = 1.63 \times 10^{-4}$), and globe width ($p = 7.0 \times 10^{-3}$). For each increase in weight of 1 kg, the globe height increased by 0.01 mm, globe length increased by 0.54 mm, and globe width increased by 0.48 mm.

Increased age was statistically associated with an increase in mean lens attenuation in H.U. ($p = 1.28 \times 10^{-7}$) and the transverse lens width ($p = 1.64 \times 10^{-3}$). For each increase in age of 1 month, the mean lens attenuation

TABLE 1 Summary of ocular structure measurements on CT for 50 rabbits with non-ocular disease.

	Right			Left			Combined		
	Mean	**SD**	**Range**	**Mean**	**SD**	**Range**	**Mean**	**SD**	**Range**
Globe length (mm)	16.54	0.68	15.12–18.56	16.75	0.63	15.37–17.98	16.64	0.66	15.12–18.56
Globe width (mm)	18.01	0.82	16.02–19.66	18.05	0.80	16.24–19.76	18.03	0.81	16.02–19.76
Globe height (mm)	17.05	0.65	15.52–18.39	17.31	0.72	15.90–19.13	17.18	0.69	15.52–19.13
Anterior chamber (mm)	2.12	0.29	1.52–2.92	2.11	0.26	1.41–2.74	2.11	0.27	1.41–2.92
Vitreous chamber (mm)	6.11	0.60	4.66–7.75	6.31	0.51	5.24–7.87	6.21	0.57	4.66–7.87
Lens length (mm)	7.84	0.43	7.04–9.07	7.86	0.47	6.21–9.21	7.85	0.45	6.21–9.21
Lens width (mm)	10.29	0.50	9.19–11.36	10.31	0.47	9.39–11.43	10.30	0.48	9.19–11.43
Vitreous attenuation (HU)	11.22	3.39	4.43–18.29	11.61	3.22	6.00–17.93	11.42	3.30	4.43–18.29
Lens attenuation (HU)	154.8	6.28	138.1–169.2	155.7	7.08	140.7–168.8	155.2	6.67	138.1–169.2

Note: Data are presented for right and left eyes individually, as well as combined across both eyes.

Abbreviations: HU, Hounsfield Units; mm, millimeters; SD, standard deviation.

TABLE 2 Summary statistics for 49 rabbits, displaying statistical significance (p-value, where a weak significance is $p < .05$, and a strong significance is $p < .01$) comparing patient characteristics against ocular biometric measurements.

***p*-value (*n* = 49)**	**Gender (male)**	**Ear conformation (upright)**	**Age**	**Weight**	**Body condition (poor)**	**Body condition (obese)**
Globe length	0.147	0.874	0.085	1.63×10^{-4}	0.786	0.054
Globe width	0.912	0.422	0.128	0.007	0.952	0.109
Globe height	0.385	0.947	0.049	2.43×10^{-5}	0.926	0.238
Anterior chamber length	0.188	0.506	0.022	0.119	0.709	0.786
Vitreous chamber length	0.040	0.628	0.690	0.034	0.686	0.186
Lens length	0.068	0.784	0.321	0.370	0.695	0.910
Lens width	0.894	0.921	1.64×10^{-3}	0.092	0.484	0.314
Vitreous attenuation	0.462	0.733	0.648	0.011	0.435	0.251
Lens attenuation	0.108	0.716	1.28×10^{-7}	0.084	0.739	0.848

increased by 0.28 H.U., representing an increase in density, and the transverse lens width increased by 0.02 mm.

Increased age was statistically associated with an increase in anterior chamber length ($p = .022$). For each increase in age by 1 month, the anterior chamber depth increased by 0.006 mm. Increased weight was statistically associated with an increase in vitreous chamber length ($p = .034$) and a decrease in mean vitreous attenuation ($p = .011$). For each increase in weight by 1 kg, vitreous chamber length increased by 0.27 mm and mean vitreous attenuation decreased by 1.56 H.U.

Male sex status was statistically associated with a decrease in vitreous chamber length ($p = .040$) of 0.30 mm compared to females. There were no statistically significant differences in ocular measurements associated with ear conformation or poor or obese body condition.

3.4 | Comparison of measurements before and after intravenous contrast administration

When comparing paired pre- and post-contrast image biometrics for both eyes combined in all 50 rabbits, statistically significant differences in measurements were identified for globe width ($p = .033$) and lens length ($p = .028$) only. There was a median reduction of −0.33 mm (range: −1.22 to +1.11 mm) between pre- and post-contrast paired measurements of globe width i.e., the post-contrast measurements were 0.33 mm smaller. The median increase between paired pre- and post-contrast lens length measurements was +0.23 mm (range: −0.40 to +0.74 mm) i.e., the lens length was measured as 0.23 mm larger in the post-contrast images.

3.5 | Intraobserver and interobserver repeatability

There was excellent intraobserver repeatability with an ICC of 0.9997, as well as excellent interobserver repeatability for all measurements with an ICC of .998. Among each observer, the measured distances of globe width, height, and length varied by up to 0.6 mm, mean attenuation of the lens varied between 140 and 168 H.U., and mean attenuation of the vitreous chamber varied between 8 and 18 H.U. for each observer.

4 | DISCUSSION

A repeatable measuring technique is described for ocular structures in rabbits, and reference values for size and attenuation are proposed. There were small but noteworthy differences between the proposed reference values on CT in this study and those reported via ultrasound by a previous study.[20] Mean anteroposterior globe length proposed on ultrasound in that study was 17.12 ± 0.41 mm. This was within 2.9% of the mean length we proposed on CT. Some other ocular biometric values established previously on ultrasound differed by these CT reference ranges by up to 12.6%. Differences in those standardized measurements are most likely attributable to differences in sample characteristics (a homogeneous population of thirty 10-month-old New Zealand white rabbits were used in that study). Alternatively, the small differences may be partially accounted for by increased spatial resolution of ultrasound imaging compared to CT. The relatively high pitch of 1.5 used to acquire the soft tissue images quickly to reduce motion artifact in the unsedated rabbit may contribute to lower CT image resolution. Ideally, the validity of all CT measurements would be assessed by comparing them to a gold standard, such as characteristics of ocular structures on necropsy, and this was not pursued in the scope of this investigation.

With increasing lean body weight, an increase in all globe measurements (length, width, and height), as well as vitreous chamber length, was observed. Similarly and unsurprisingly, in a study describing canine CT ocular biometrics, globe dimensions were also found to statistically significantly increase with weight.[13] Body condition score did not statistically significantly affect any ocular measurements, and so it is less likely that ocular dimensions are altered by fat-deposition related compression of ocular structures, and more likely that the difference observed with increasing weight is a consequence of larger anatomical body dimensions.

As age increased, so did the mean lens attenuation in H.U. and transverse lens width (equatorial diameter). By including rabbits between the ages of 18 and 78 months, we sought to concurrently avoid age-related growth as a variable for increased globe dimensions (minimal globe growth has been described beyond 18 months of age),[21–23] while minimizing degenerative changes in aging rabbits, while including a heterogeneous population that is representative of that encountered in clinical practice. It has been found that minimal lens growth may continue up to and possibly beyond 4 years of age. An increase in lens attenuation with age occurs due to the continual development of lens fibers throughout a rabbit's life, and this is proposed to also increase transverse lens width.[24,25] Furthermore, it has been demonstrated that the lens becomes stiffer with increasing age in rabbits,[26] decreasing the accommodating ability of the lens,[27,28] which may contribute to the increase in

lens width with age—a less compliant lens will retain a relatively flattened, oblate spheroidal shape.[27] This same principle may account for the increase in anterior chamber length with age; the lens retains a flattened shape, bulging less into the anterior chamber. It is important to bear in mind that the measurements on CT are not correlated to the actual size of the lens in this study once it has been removed. Rabbits younger than 18 months were not included in this study, and so the described reference ranges likely differ in younger rabbits that are not skeletally mature.

Males had a smaller vitreous chamber length than females. The relationship between male sex and smaller vitreous chamber length may be attributable to sample characteristics and a possible disproportion in the included weight of male and female rabbits. The possibility of sex-related morphological differences is something that can be investigated in future anatomic studies. As rabbit weight increased, there was a statistically significant increase in vitreous chamber length and a decrease in mean vitreous attenuation. The degree of these differences was miniscule, with an increase in vitreous chamber length of only 0.27 mm per kilogram, and a small decrease in attenuation by 1.56 H.U. per kilogram. Each of these findings are so small in scale that they are not clinically significant. As age increased, there was a statistically significant increase in globe height. Whether this is attributable to age-related globe compliancy changes, or is due to a small sample size, needs to be investigated further.

There was no correlation between left and right mean vitreous attenuation; in other words, as a change in attenuation was present in one side, a corresponding change was not present in the other. The difference in the mean vitreous attenuation among each eye may be attributable to degenerative changes happening at a different rate in each eye, as it has been observed on post mortem examination that the rabbit vitreous body undergoes liquefaction (typically subclinical degeneration) from an early age.[29] Alternatively, the difference may be artifactual as attenuation measurements can be greatly affected by subtle beam hardening even if care was taken to avoid it when visible. It is worth noting that these differences in attenuation are not grossly appreciable on CT, and to our knowledge, it has not been demonstrated that vitreous liquefaction is able to be appreciated on CT. The heterogeneous composition of vitreous humor (a transparent gelatinous mass composed of water, collagen fibrils, hyaluronic acid, hyalocytes, inorganic salts, sugar and ascorbic acid) has been described to contribute to a wide range of density measurements and broad normal variation.[16]

Intravenous contrast administration resulted in a statistically significant decrease in the globe width and an increase in the anteroposterior length of each lens. Globe width was measured from the internal surface of the choroid-retina-sclera complex to the internal margin of the choroid-retina-sclera complex on the other side of the globe. Increased attenuation of the enhancing choroid may decrease the apparent width of the globe via blooming artifact. It would be expected that the globe height would also be affected by this, as it too is bound on each end by the enhancing choroid. Regarding the apparent increase in lens length, it is possible that contrast administration decreased perceptible spatial resolution as the contrast increases the total object contrast range, thereby making the lens appear larger. However, the median difference in lens length after contrast administration is minute at 0.23 mm and the median difference in globe width was only 0.33 mm. These are less than the CT slice thickness of 1.0 mm and are therefore unlikely to be clinically relevant.

A CT reference range may be used to aid in identification of conditions that result in alteration of the dimensions or attenuation of ocular structures, such as buphthalmos secondary to glaucoma, especially in cases where ciliary bodies have degenerated, and intraocular pressure has normalized, and is therefore not identified on clinical examination. A reference range may aid in identifying buphthalmia, especially when present bilaterally, where comparison to a presumably normal contralateral eye is not possible.

There were limitations owing to the retrospective nature of this study. The eyes of each patient were assessed on clinical exam by exotics clinicians, however a full ophthalmologic examination by a board-certified ophthalmologist was not performed. Histopathology was not performed to confirm absence of ocular disease, or to correlate the distances measured with the true size of the structures. Therefore, ocular pathology which may affect the dimensions and attenuation of structures of the globe were not definitively excluded. The presence of subtle nuclear sclerosis could increase attenuation of the lens and may account for the increased mean attenuation of the lens with age. Similarly, intraocular pressure was not determined in these patients, and so glaucoma was not definitively excluded.

Although a consistent method was followed to rotate the eye around its center into the three different planes, the measurements were made by visual judgment of the greatest dimension and are therefore subject to a degree of human error. Intra and interobserver agreement was evaluated on only a subset of cases. In this subset, intra- and interobserver agreement was excellent, demonstrating the repeatability of the measurement protocol. A

comparable subset of cases has been used to assess inter and intra observer variability in other studies.[13]

In conclusion, CT is a reliable imaging modality for assessing ocular dimensions in rabbits. This study serves to provide baseline biometric CT measurements in rabbits greater than 18 months of age, without reported ophthalmologic abnormalities.

AUTHOR CONTRIBUTIONS

Nicholas Goody: Investigation; methodology; project administration; writing – original draft; writing – review and editing. **Nicolas Israeliantz:** Conceptualization; data curation; investigation; methodology; project administration. **Azzurra Massidda:** Conceptualization; methodology. **Jenna Richardson:** Conceptualization; data curation; investigation; methodology. **Benjamin Blacklock:** Conceptualization; methodology. **Jordan Mitchell:** Formal analysis. **Tiziana Liuti:** Data curation; investigation; methodology; project administration.

CONFLICT OF INTEREST STATEMENT

The authors have no potential conflicts of interest to declare concerning the research, authorship, and/or publication of this article.

DATA AVAILABILITY STATEMENT

Data available on request from the authors.

ETHICS STATEMENT

This study was approved by the Veterinary Ethical Review Committee of The Royal (Dick) School of Veterinary Studies. Animal owners or owners' representatives provided written informed consent for enrollment in the study, procedures and therapy undertaken, and publication of data and images.

ORCID

Nicholas Goody https://orcid.org/0000-0002-1174-5409
Nicolas Israeliantz https://orcid.org/0000-0002-8472-094X
Azzurra Massidda https://orcid.org/0000-0002-0945-811X

REFERENCES

1. Sánchez-Vizcaíno F, Noble PM, Jones PH, et al. Demographics of dogs, cats, and rabbits attending veterinary practices in Great Britain as recorded in their electronic health records. *BMC Vet Res*. 2017;13(1):218. doi:10.1186/s12917-017-1138-9
2. Zernii EY, Baksheeva VE, Iomdina EN, et al. Rabbit models of ocular diseases: new relevance for classical approaches. *CNS Neurol Disord Drug Targets*. 2016;15(3):267-291. doi:10.2174/1871527315666151110124957
3. Barathi A, Thu MK, Beuerman RW. Dimensional growth of the rabbit eye. *Cells Tissues Organs*. 2002;171(4):276-285. doi:10.1159/000063123
4. Peiffer RL Jr, Pohm-Thorsen L, Corcoran K. Models in ophthalmology and vision research. *The Biology of the Laboratory Rabbit*. Elsevier Inc; 1994:409-433.
5. Ohlerth S, Scharf G. Computed tomography in small animals—basic principles and state of the art applications. *Vet J*. 2007;173(2):254-271. doi:10.1016/j.tvjl.2005.12.014
6. Boehler A, Henninger W. Computed tomography of the rabbit head without general anaesthesia. *Wien Tierarztl Monatsschr*. 2008;95:116-120.
7. Van Caelenberg AI, De Rycke LM, Hermans K, et al. Computed tomography and cross-sectional anatomy of the head in healthy rabbits. *Am J Vet Res*. 2010;71(3):293-303. doi:10.2460/ajvr.71.3.293
8. Riggs GG, Arzi B, Cissell DD, et al. Clinical application of cone-beam computed tomography of the rabbit head: part 1—normal dentition. *Front Vet Sci*. 2016;3:93. doi:10.3389/fvets.2016.00093
9. Richardson J, Longo M, Liuti T, et al. Computed tomographic grading of middle ear disease in domestic rabbits (*Oryctolagus cuniculi*). *Vet Rec*. 2019;184(22):679. doi:10.1136/vr.104980
10. Artiles CA, Sanchez-Migallon Guzman D, Beaufrère H, Phillips KL. Computed tomographic findings of dental disease in domestic rabbits (*Oryctolagus cuniculus*): 100 cases (2009–2017). *J Am Vet Med Assoc*. 2020;257(3):313-327. doi:10.2460/javma.257.3.313
11. Palma-Medel T, Marcone D, Alegría-Morán R. Dental disease in rabbits (*Oryctolagus cuniculus*) and its risk factors-a private practice study in the metropolitan region of Chile. *Animals*. 2023;13(4):676. doi:10.3390/ani13040676
12. Thrall DE, Robertson ID. Chapter 2—the skull. *Atlas of Normal Radiographic Anatomy and Anatomic Variants in the Dog and Cat*. 2nd ed. W.B. Saunders; 2016 21.
13. Chiwitt CLH, Baines SJ, Mahoney P, et al. Ocular biometry by computed tomography in different dog breeds. *Vet Ophthalmol*. 2017;20(5):411-419. doi:10.1111/vop.12441
14. Chandrakumar SS, Zur Linden A, Owen M, et al. Computed tomography measurements of intraocular structures of the feline eye. *Vet Rec*. 2019;184(21):651. doi:10.1136/vr.105136
15. Hollis AR, Dixon JJ, Berlato D, Murray R, Weller R. Computed tomographic dimensions of the normal adult equine eye. *Vet Ophthalmol*. 2019;22(5):651-659. doi:10.1111/vop.12636
16. Salgüero R, Johnson V, Williams D, et al. CT dimensions, volumes and densities of normal canine eyes. *Vet Rec*. 2015;176(15):386. doi:10.1136/vr.102940
17. Gumpenberger M, Kolm G. Ultrasonographic and computed tomographic examinations of the avian eye: physiologic appearance, pathologic findings, and comparative biometric measurement. *Vet Radiol Ultrasound*. 2006;47(5):492-502. doi:10.1111/j.1740-8261.2006.00168.x
18. Künzel F, Hittmair KM, Hassan J, et al. Thymomas in rabbits: clinical evaluation, diagnosis, and treatment. *J Am Anim Hosp Assoc*. 2012;48(2):97-104. doi:10.5326/jaaha-ms-5683
19. Schober P, Boer C, Schwarte LA. Correlation coefficients: appropriate use and interpretation. *Anesth Analg*. 2018;126(5):1763-1768. doi:10.1213/ane.0000000000002864

20. Toni M, Meirelles A, Gava F, et al. Rabbits' eye globe sonographic biometry. *Vet Ophthalmol*. 2010;13(6):384-386. doi:10.1111/j.1463-5224.2010.00831.x
21. Sarnat B. Orbital volume after enucleation and eye volume in the adult rabbit. *Albrecht Von Graefes Arch Klin Exp Ophthalmol*. 1978;208(4):241-245. doi:10.1007/BF00419379
22. Bozkir G, Bozkir M, Dogan H, Aycan K, Güler B. Measurements of axial length and radius of corneal curvature in the rabbit eye. *Acta Med Okayama*. 1997;51(1):9-11. doi:10.18926/amo/30804
23. Holmberg BJ. Ophthalmology of exotic pets. *Slatter's Fundamentals of Veterinary Ophthalmology*. Elsevier Inc; 2008:427-441.
24. Al-khudari S, Donohue ST, Al-Ghoul WM, et al. Age-related compaction of lens fibers affects the structure and optical properties of rabbit lenses. *BMC Ophthalmol*. 2007;7(1):19. doi:10.1186/1471-2415-7-19
25. Michael R, Bron AJ. The ageing lens and cataract: a model of normal and pathological ageing. *Philos Trans R Soc Lond Ser B Biol Sci*. 2011;366(1568):1278-1292.
26. Zhang X, Wang Q, Lyu Z, et al. Noninvasive assessment of age-related stiffness of crystalline lenses in a rabbit model using ultrasound elastography. *Biomed Eng Online*. 2018;17(1):75. doi:10.1186/s12938-018-0509-1
27. Reilly MA. A quantitative geometric mechanics lens model: insights into the mechanisms of accommodation and presbyopia. *Vis Res*. 2014;103:20-31. doi:10.1016/j.visres.2014.08.001
28. Weeber HA, van der Heijde RGL. On the relationship between lens stiffness and accommodative amplitude. *Exp Eye Res*. 2007;85(5):602-607.
29. Los LI. The rabbit as an animal model for post-natal vitreous matrix differentiation and degeneration. *Eye*. 2008;22(10):1223-1232. doi:10.1038/eye.2008.39

How to cite this article: Goody N, Israeliantz N, Massidda A, et al. Ocular biometry in rabbits using computed tomography. *Vet Ophthalmol*. 2024;00:1-10. doi:10.1111/vop.13209